Biomass and Bioenergy 158 (2022) 106349

Contents lists available at ScienceDirect

Biomass and Bioenergy

journal homepage: www.elsevier.com/locate/biombioe

A hybrid of response surface methodology and artificial neural network in optimization of culture conditions of mycelia growth of *Antrodia cinnamomea*

Meng-Hsin Lee [a], Wei-Bin Lu [b], Mei-Kuang Lu [c,d,*], Fi-John Chang [a,**]

[a] Department of Bioenvironmental Systems Engineering, National Taiwan University, No. 1, Sec. 4, Roosevelt Rd, Taipei, 10617, Taiwan
[b] Department of Cosmetic Science, Chung Hwa University of Medical Technology, No. 89, Wunhwa 1st St, Tainan, 71703, Taiwan
[c] National Research Institute of Chinese Medicine, Ministry of Health and Welfare, 155-1 Li-Nung St., Sec. 2, Shipai, Peitou, Taipei, 11221, Taiwan
[d] Graduate Institute of Pharmacognosy, Taipei Medical University, 252 Wu-Hsing St., Taipei, 11031, Taiwan

ARTICLE INFO

Keywords:
Antrodia cinnamomea
Biomass production
Mycelia growth
Response surface methodology (RSM)
Artificial neural network (ANN)

ABSTRACT

Antrodia cinnamomea (*A. cinnamomea)* faces the challenge of coping with commercial usage in formulating nutraceuticals and functional foods in Taiwan. This research aimed to increase the biomass production of mycelia during the cultivation of *A. cinnamomea* using a methodology that hybrids Response Surface Methodology (RSM) and Artificial Neural Network (ANN). RMS aimed to optimize the culture condition while ANN intended to identify the factors dominating biomass production. The Plackett-Burman design and 32 (2^{7-2}) fractional factorial designs identified four key factors. A four-factor six-level central composite design was used to investigate the correlation between the biomass and the key factors. The yield of RSM was 200% higher than that of the control medium. The proposed methodology offers reliable production of the medicinal fungus under optimum conditions in laboratory culture and reduces the cost, time and effort made, compared to the slow-growing propagation in nature. ANN opens a new opportunity of biomass prediction in microbial cultivation. Moreover, we provide the potential of hybrid RSM-ANN methods when encountering multifarious tasks in the future with the hope of bringing forward a new generation of biomass production technologies.

1. Introduction

In the current scenario, the under exploitation of bio-resources and increasing economical requirements force scientific communities to search for alternative renewable bio-resources like biomass-derived energy to achieve the Sustainable Development Goals [1]. Under this scenario, through obtaining bioactive compounds from mushrooms, submerged cultures have the potential for high-yield and high-quality mycelial production in a compact space with fewer chances for contamination within a shorter time. Currently available reports on nutritional requirements in cultures are limited to only a few mushrooms, *ie. Antrodia cinnamomea* (*A. cinnamomea)* [2–4], *Ganoderma lucidum* [5], and *Paecilomyces japonica* [6]. Unlike many efforts that have been made to explore the optimal submerged culture conditions for the production of biomass and secondary metabolites from several mushrooms, a hybrid ANN & RSM approach offers the potential for a multitude of economic and environmental benefits [7].

A. cinnamomea, a medicinal and slow-growing fungus and commonly known as 'niu-chang chih' or 'jang-jy', has been used for illness caused by toxication, such as by alcohol, food, or drugs, as well as for skin itching, cancer, anti-aging, diarrhea, abdominal pain, and hypertension [8,9]. *A. cinnamomea* is an indigenous fungus that parasitizes on the inner cavity of *Cinnamomum kanehirae*, an endemic species in Taiwan. Due to the limited distribution of the host plant and the slow-growing rate in nature, researchers have made attempts to mass produce the entitled fungus through fermentation systems for pharmaceutical usage [10]. We have successfully used the precursor-feeding strategy for mass producing the sulfated polysaccharides of this fungus, including microelement [11], sodium thiosulfate [12], and ammonium sulfate [13]. The polysaccharides from the cultured mycelia of the fungus display anti-cancer activity [14] and anti-inflammatory activity [13].

Our previous studies indicated the mycelial growth of *A. cinnamomea*

* Corresponding author. National Research Institute of Chinese Medicine, Taipei, Taiwan.
** Corresponding author. Department of Bioenvironmental Systems Engineering, National Taiwan University, Taipei, Taiwan.
E-mail addresses: mklu@nricm.edu.tw (M.-K. Lu), changfj@ntu.edu.tw (F.-J. Chang).

https://doi.org/10.1016/j.biombioe.2022.106349
Received 10 August 2021; Received in revised form 6 December 2021; Accepted 9 January 2022
Available online 18 January 2022

may be affected by several independent factors such as glucose, potato dextrose broth (PDB), *Cinnamomea camphora* (CC)-polysaccharide (PS), CC water extract, agar, and the culture condition of pH [15–17], where these factors were investigated based on one-factor-at–a-time experiments. Documentation concerning how several factors affect the mass production of this species is rare. The Response Surface Methodology (RSM), a statistical approach introduced by Box and Wilson [18], can effectively explore the relationships between several explanatory variables and response variables and has been widely employed to maximize the production of a specific substance by optimizing operational factors [19,20]. There are also reports on the optimization of culture conditions using RSM for the growth of fungal species from different sources [21–23]. Artificial neural networks (ANNs) can extract the nonlinear relationship between input and output variables for modelling nonlinear problems and have been broadly used in various disciplines of scientific research, such as biomass estimation [24–26], biofuel production [27,28], and environmental issues [29–32]. Therefore, ANNs are considered to be potential tools to estimate the optimum culture conditions for biomass production of mycelia [33]. Nevertheless, there is very limited documentation available in the application of ANNs to biomass production [34,35]. Researchers have paid much attention to using ANNs for the classification and/or estimation of biomass and bioethanol production [36–38]. It is therefore worthwhile investigating the optimization of the growth conditions of *A. cinnamomea* by use of RSM and ANN.

Our previous study cultured the parasitic hypha of *A. cinnamomea* in the presence of water-soluble wood extracts from the host and four host-related species (*C. kanehirae, C. micranthum, C. osmophloeum, C. camphora, and C. kotoense*), and the results indicated that *C. cinnamomea* (CC) water extract exhibits a higher level of growth promotion activity than its host [17]. The effect of camphor concentration on the growth of *A. cinnamomea* was reported [39]. This study propose a methodology integrating RSM and ANN to identify the key affecting factors from CC water extract and six other variables as well as optimize the mycelial growth of *A. cinnamomea* during cultivation. We next demonstrate the effectiveness and suitability of the proposed methodology for enabling reliable production of the medicinal fungus under optimum conditions in laboratory culture.

2. Materials and methods

2.1. Shake-flask culture of A. cinnamomea

The *A. cinnamomea* isolate (strain B85) obtained from Taitung County in Taiwan was a generous gift from Dr. T.T. Chang (Division of Forest Protection, Forest Research Institute, Taipei, Taiwan). *A. cinnamomea* was subcultured and maintained in essentially the same manner as reported previously [16]. Briefly, *A. cinnamomea* was inoculated at the center of Petri dishes containing 39 g/L of potato dextrose agar at 28 °C for 19 days before being transferred to liquid culture. The initial medium for liquid culture contained 40.00 g/L of PDB, 20.00 g/L of glucose, 0.16 g/L of CC-PS, 1.00 g/L of camphor, 20.00 g/L of CC water extract, 2.00 g/L of agar, and a pH value of 5.60, which was denoted as the "start point". The various conditions were incubated at the corresponding dosages or condition for another 7 days by shaking at 50 rpm to obtain a mucilaginous medium containing mycelia. At the end of the incubation, the mycelia were rapidly washed with 1 L of NaCl (250 mM) using an aspirator-suction system to remove the contaminated culture medium. Samples were then lyophilized, and the dry weight of the mycelia was recorded.

2.2. Experimental design

2.2.1. Optimization of growth conditions for biomass production

Various physic-chemical factors were considered to improve the mycelial growth of *A. cinnamomea*. Among different physic-chemical parameters, some important parameters (variables) were chosen for use in the optimization process of the culture condition. The optimization experiments were carried out in triplicate. The initial and important step in the optimization process consisted of the design of the experiment and the selection of each variable's range. Multiple variables were involved, and the yield was considered to be the response of independent factors. RSM was used to identify the optimum conditions for the process response. It, however, was a time-consuming and laborious experimental process to identify the important factors affecting the process response using RSM methods. Therefore, we used an ANN fed with the first-stage RSM results as input data to efficiently and effectively identify the dominant factors for biomass production.

2.2.2. Response surface methodology (RSM)

To investigate the interactive effects of the seven variables, including pH (X_1), glucose (X_2), PDB (X_3), CC-PS (X_4), camphor (X_5), CC water extract (X_6), and agar (X_7), on biomass production, we employed two-level fractional factorial designs (i.e. a 2^{7-2} design has 32 runs), a method commonly adopted by RSM, to identify the non-significant factor(s) of the mycelial growth condition and reasonably reduce the number of experiments without affecting the acquisition of information. The experimental design for the seven factors (X_1-X_7) is described in Supplementary Tables S–1, followed by performing the steepest ascent method (SAM) to make the concentration of each factor approach the range where the extreme point is located. Finally, the central composite design (CCD) was used to explore the regression equation for estimating the curvature of the yield and each factor based on the central point (from the fractional factorial design) coupled with the star point.

2.2.2.1. Steepest ascent method (SAM). When many variables are involved, a two-level fractional factorial design can well determine the path of steepest ascent toward the neighborhood of the response optima. SAM will then be employed to reach the neighborhood of the center point of the Plackett-Burman design (PBD) space, which can be considered to be the origin for SAM (Supplementary Tables S–2). In this study, experiments were run along the path described by SAM [40].

2.2.2.2. Central composite design (CCD). CCD, a second-order experimental design, was then employed to fully elucidate the response surface near the optimum that provided a basis for the second-order polynomial approximation to the true response. In this study, CCD consisted of four factors (X_1, X_2, X_3, and X_7) and each factor had five code levels (−2, −1, 0, 1, and 2). The levels of independent variables were: 5–8.7 for pH; 0.600–0.652 g/30 mL for glucose; 1.200–1.250 g/30 mL for PDB; and 0.060–0.138 g/30 mL for agar. A total of 26 runs were generated using Design Expert, where 16 runs were factorial runs, 8 runs were axial runs, and 2 runs were for replicating the center point. The other three factors were held constant at the central point of the PBD space.

The quality of the fitted polynomial model was assessed by the coefficient of determination (R^2). According to the experimental data, mathematical models were established based on initial pH values and C-source concentrations via multiple regression, and then they were used to resolve the maximum by partial differentiation for obtaining the new center point for the process response of the next step (T4 experiment in this study). This study fitted a full second-order regression model (Eq. (1)) to the experimental data for determining its coefficients.

$$Y = a_0 + a_1X_1 + a_2X_2 + a_3X_3 + a_4X_4 + a_{12}X_1X_2 + a_{13}X_1X_3 + a_{14}X_1X_4 + a_{23}X_2X_3 + a_{24}X_2X_4 + a_{34}X_3X_4 + a_{11}X_1^2 + a_{22}X_2^2 + a_{33}X_3^2 + a_{44}X_4^2 \quad (1)$$

where Y is the expected response value predicted by RSM; and a_i, a_j and a_{ij} are the model parameters to be estimated.

In this study, the multiple regression analysis was used to evaluate the experimental data, with significance judged by the *p* value. All of the regression planes were generated and analyzed by the software "JMP statistical software package" (SAS Institute Inc., USA).

2.3. Self-organizing feature map (SOM)

An artificial neural network (ANN) is an algorithm performed by mathematically modeling the interconnected network structure for simulating human neural networks and is considered an effective tool for modeling biomass production (Fig. 1). The self-organizing feature map (SOM) belongs to the family of ANNs and was used in this study for identifying the factors dominating the growth of *A. cinnamomea*. SOM contains several nodes, and associated with each node are the clustered input data (variables) and a position in the map space [41]. SOM is commonly constructed into a two-dimensional grid that represents a lattice-like structure among neurons (nodes) to form a topological map for visualizing data characteristics. SOM learns to recognize the groups of similar input vectors in such a way that neurons physically near each other in the hidden layer respond to similar input vectors. Each neuron contains a vector with the same dimension of the input vector. Neurons are subsequently trained based on competitive learning [42,43], which can convert multi-dimensional input patterns into the responses of two-dimensional ordering of neurons through performing this transformation adaptively in a topologically ordered fashion. Consequently, SOM enables the detection of the inherent structure and the interrelationship of input data. Fig. 2 presents the architecture of SOM, consisting of input variables, winner-clustered hidden nodes, and the weighted sum of the outputs.

The 32 data sets of fractional factorial designs (T1) were used as the training data for SOM. The implementation steps of the training algorithm for SOM are summarized as follows.

Step 1. The initial training stage, initialize the weights of neurons with random values.
Step 2. Find a neuron (denoted as the winner) with a weight vector the most similar to the input vector (variables) according to the minimum distance Euclidean criterion.
Step 3. Adjust the weights of the winner and its neighborhood neurons towards the input vector. The magnitude of the change decreases with the distance from the winner over time.

This training process repeats until the feature map (topology) is well unfolded. If the map fails to be unfolded after a certain number of iterations (e.g., 2000), it is suggested restarting the training process with a different set of initial weights. Following the training process, the obtained topology displays the neurons on the grid in topological order so similar neurons stay close to one another while dissimilar neurons stay far from each other. Consequently, input vectors (training samples) are allocated into the constructed topological map based on the degree of similarity.

SOM uses an unsupervised learning algorithm to group input data into clusters of similar patterns, and therefore input vectors can memorize the clustering results specific to the network only. This behavior can benefit the recognition of the problem but cannot effectively reach a continuous function approximation. It is noted that similar input patterns may result in different outputs. Therefore, it is common to use the average of output values as the input patterns clustered into the corresponding neuron, followed by using the output of the closest (the most similar) neuron directly for the given input pattern [29,44].

3. Results and discussion

In this study, 4-stage experiments (T1-T4) were conducted by RSM, with each culture condition being performed in triplet. A total of 96-, 18-, 78- and 6-run experiments were carried out in T1-T4, respectively. In support of factor analysis, SOM based on the T1 results of RSM was responsible for efficiently and effectively identifying the dominant factors for biomass production. According to the single-factor analysis, process variables and their ranges were selected while independent variables were coded at three levels between −1 and 1 (Table 1).

3.1. SOM for the identification of dominant factors

SOM can effectively group input vectors into clusters of similar patterns. One of its most significant features and contributions is the results obtained from SOM can be visualized on its topological map. Once the structure of SOM is determined, it stores the most relevant information of the input variables in its topological map and allows all such information to be displayed and explored. This study used SOM to cluster the biomass obtained from the liquid culture process (T1). The input layer of SOM contained the culture conditions of seven parameters (variables), namely pH, glucose, PDB, CC-PS, camphor, CC water extract, and agar. Due to the limited number (32 in this study) of samples, only a few map sizes of SOM were conducted to determine the most suitable network structure (i.e. the number of neurons in the hidden layer). After a number of trials, a total of 9 neurons in a hidden layer were determined and the output was composed of one projected variable (biomass production). It is noted that the input variables were normalized before training the network. The weights and biases were adjusted by the SOM algorithm. In this study, the 32 datasets (samples) were

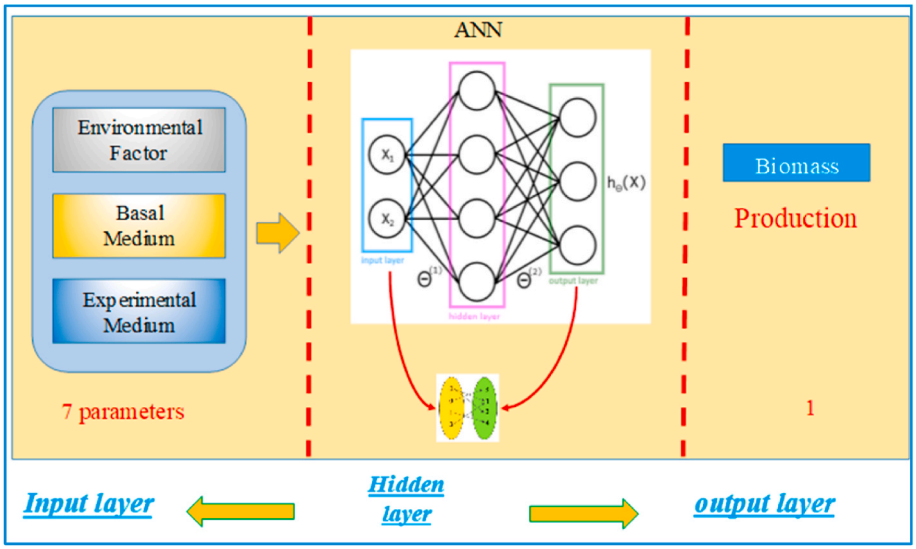

Fig. 1. Scheme of the artificial neural network (ANN) for modelling biomass production.

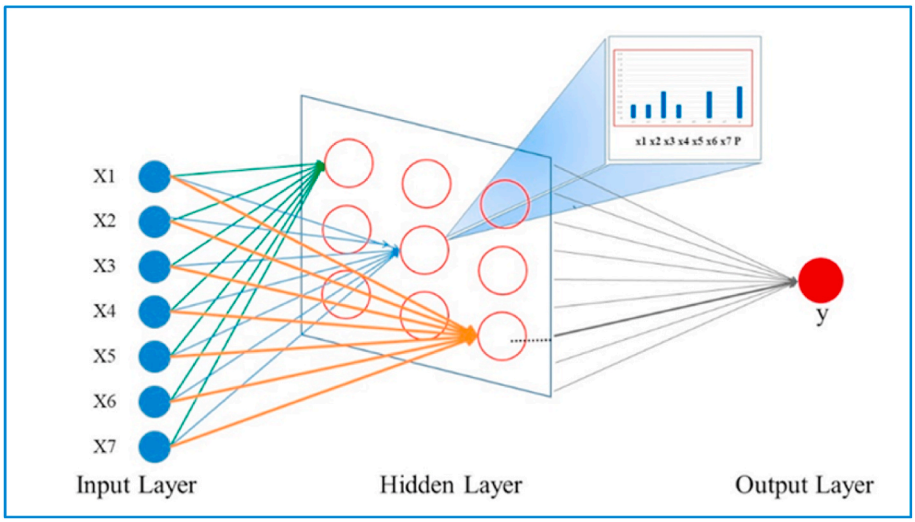

Fig. 2. Architecture of the self-organizing map (SOM) for clustering the input variables.

Table 1
Assigned concentration of each variable at different levels and spacing of levels expressed in coded and natural units.

Independent variables		Code levels		
		−1	0	+1
X_1	pH	4.6	5.6	6.6
X_2	Glucose (g/L)	0	20	40
X_3	PDB (g/L)	30	40	50
X_4	CC polysaccharides (g/L)	0	0.16	0.32
X_5	Camphor (g/L)	0	1	2
X_6	CC water extract (g/L)	10	20	30
X_7	Agar (g/L)	0	2	4

clustered by the Neural Net Clustering (SOM) of MATLAB (Version 2019a) based on 600 training epochs.

The samples in each of the 9 clusters are listed in Supplementary Tables S–3. Cluster 1 (containing samples #18, #19, #25 and #28) had the maximal mean value of the biomass while Cluster 4 (containing samples #21, #24, #30 and #31) had the minimal mean value of the biomass. The SOM results implied the clusters with larger mean values possessed more applicable culture conditions than those of smaller mean values. Fig. 3 illustrates the SOM clustering results in view of variables X_1–X_7. It appears the concentrations of X_3 (PDB) and X_7 (Agar) had a positive relation with the biomass, whereas those of X_5 (Camphor) and X_6 (CC water extract) had no relation with the biomass. Besides, it was difficult to relate X_1 (pH), X_2 (glucose) or X_4 (CC-PS) with biomass production. The SOM results suggest X_3 (PDB) and X_7 (Agar) are the dominant factors for biomass production while X_5 (Camphor) and X_6 (CC water extract) are not necessarily important for biomass production.

We further explore the constructed topological map obtained from SOM in view of 9 clusters, as shown in Fig. 4. The maximal mean value of biomass production occurred in Cluster 1, which showed X_3 (PDB) and X_7 (Agar) had the highest frequency of occurrence (i.e. each occurred 4 times; the largest red squares) in the code level of +1 while X_5 (Camphor) and X_6 (CC water extract) had the highest frequency of occurrence (i.e. each occurred 4 times; the largest grey squares) in the code level of −1. In contrast, the minimal mean value of biomass production occurred in Cluster 4, which showed X_3 (PDB), X_5 (Camphor), X_6 (CC water extract) and X_7 (Agar) had the highest frequency of occurrence (i.e. each occurred 4 times; the largest grey squares) in the code level of −1. The results suggest X_3 (PDB) and X_7 (Agar) are the dominant factors for biomass production. Specifically, it is of great potential to reach the highest biomass production when the code levels of X_3 (PDB) and X_7 (Agar) are +1 during cultivation. Nevertheless, X_5 (camphor) and X_6 (CC water extract) are considered the least important for biomass production because they were only present at the code level of −1 in both Cluster 1 (the maximal mean value of biomass) and Cluster 4 (the minimal mean value of biomass), which raises the difficulty in highlighting their importance in biomass production. As for X_1 (pH), X_2 (glucose) and X_4 (CC-PS), they did not show consistent behavior in biomass production. Therefore, further exploration of the three factors can be made by RSM.

3.2. Plackett-Burman design (PBD) for the optimization of medium composition

This study developed a hybrid methodology for optimizing the growth condition of *A. cinnamomea*. After a series of preliminary experiments, the initial pH value, glucose, PDB, CC-PS, camphor, CC water extract, and agar were determined as the potential factors affecting the growth of *A. cinnamomea*. Then, RSM was used to evaluate the relations existing between the seven experimental factors and the observed biomass. The code levels of the seven variables were selected for biomass production based on the results obtained from the conventional one-factor-at-a-time approach.

After defining the domain for each of the seven variables, the relation between these assigned values in each code level can simply be obtained from the following formula.

$$Z = \frac{(X - X^0)}{\Delta X} \quad (2)$$

where Z is the code value; X is the corresponding natural value; X^0 is the natural value in the center of the domain; and ΔX is the increment of X corresponding to one code level of Z.

Table 1 shows the experimental variables and spacing of levels expressed in coded and natural units. Supplementary Tables S–1 depicts a 2^{7-2} fractional factorial design and the results of the PBD matrix. The experiments contained variables X_1−X_7 and 32 runs of the two-level fractional factorial design and PBDs to screen the factors that were considered potential, and then the incubation was carried out for 7 days. In the experimental designs, the dry weight (biomass) of the mycelia was measured.

According to the code level and the corresponding value, 96-run experiments were conducted. The data on the biomass production of *A. cinnamomea* were presented in yield (experimentally determined biomass (g/L) after 7 days of incubation). The two-level results were regarded as the coefficients of X_1−X_7 in the first-order regression

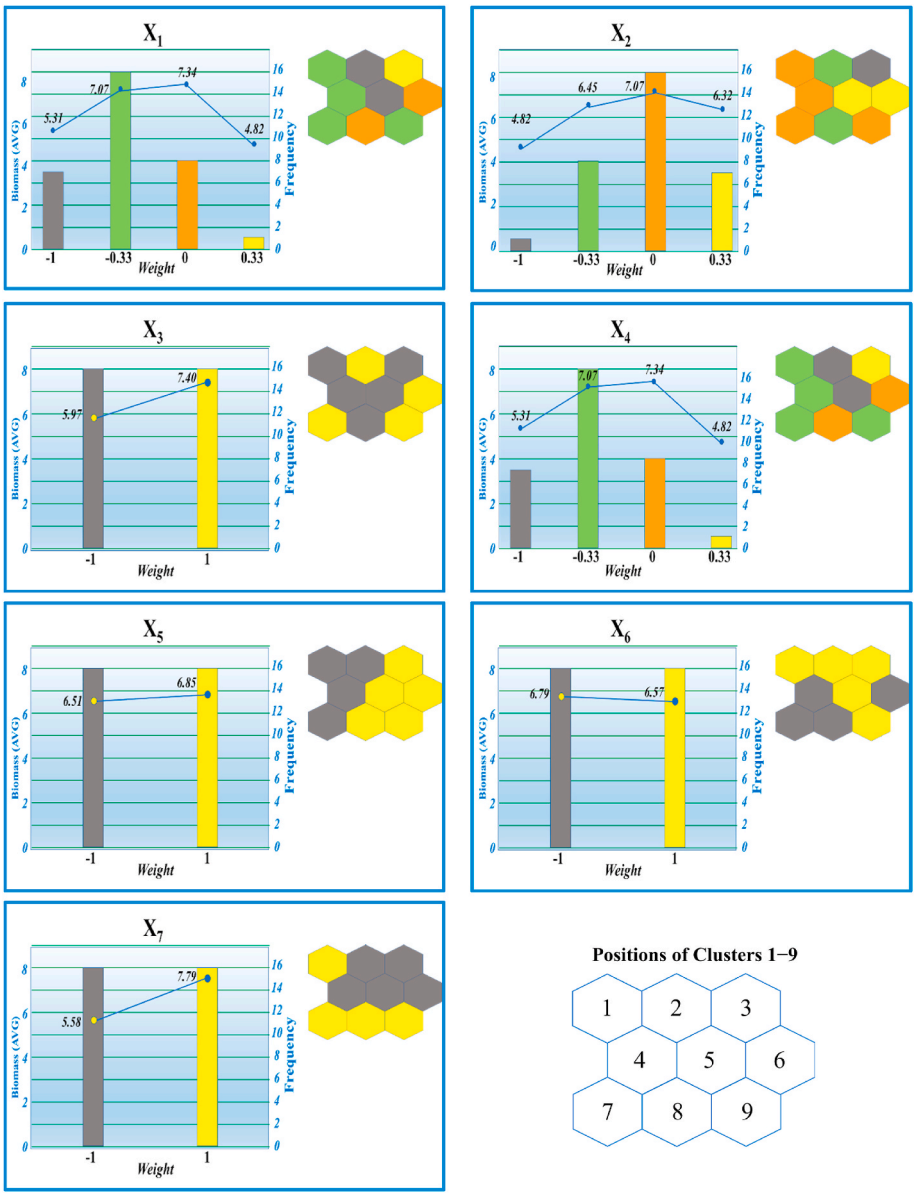

Fig. 3. SOM clustering results in view of variables X_1–X_7. The histograms express the occurrence frequencies of the weights of input data (X_1–X_7), and the curve expresses the mean value of biomass production. The upper right corner of each subfigure is the SOM topological map that shows the weight plane of each input (X_1–X_7).

equation of the fractional factorial design experiment (Table 2), along with the assigned value of each variable's path of steepest ascent (Supplementary Tables S–2). The R^2 of the regression analysis performed by the nonlinear regression of SigmaPlot 11.0 was 0.5155 (Table 2). The correlation between the observed values and the results of the screening model appeared to be highly significant (p value < 0.05), representing the actual relationship between the response (biomass) and the variables is significant. Variables pH (X_1), glucose (X_2), PDB (X_3) and agar (X_7) showed significance values of $p < 0.01$ or $p < 0.001$ and were considered to be key factors in the following design for the path of steepest ascent. The regression equation considering all the terms irrespective of their significance (expressed in terms of actual concentration values) is shown in Eq. (3).

$$Y = -5.7475 + 1.5886X_1 + 0.0366X_2 + 0.0701X_3 - 0.0822X_4 + 1.5935X_5 - 0.0124X_6 + 0.5459X_7 \quad (3)$$

where Y is the predicted mycelial biomass (g/L); X_1 is the initial pH in code form; X_2 is the concentration of glucose (g/L) in code form; X_3 is the concentration of PDB (g/L) in code form; and X_7 is the concentration of agar (g/L) in code form. The growth response will be increased by 1.5886 g/L if X_1 (initial pH) is increased by one unit. Similarly, the growth response will be increased by 0.0366 g/L if X_2 (the concentration of glucose) is increased by one unit. The growth response will be increased by 0.0701 g/L if X_3 (the concentration of PDB) is increased by one unit. The growth response will be increased by 0.5459 g/L if X_7 (the concentration of agar) is increased by one unit.

The non-significant factors from Table 3 consisted of X_4 (CC-PS), X_5 (camphor), and X_6 (CC water extract), which were discarded prior to the next design for the path of steepest ascent. In contrast, X_1 (pH), X_2 (glucose), X_3 (PDB) and X_7 (agar) were used to perform the design for the path of steepest ascent. In general, higher biomass fermentation depends on the species, cultural medium, cultural temperature, pH, dissolved oxygen, and the amount of inoculum. The carbohydrate required in culture media is usually acting as osmotica and help maintain an osmotic potential in the culture medium useful to cell and tissue growth [45].

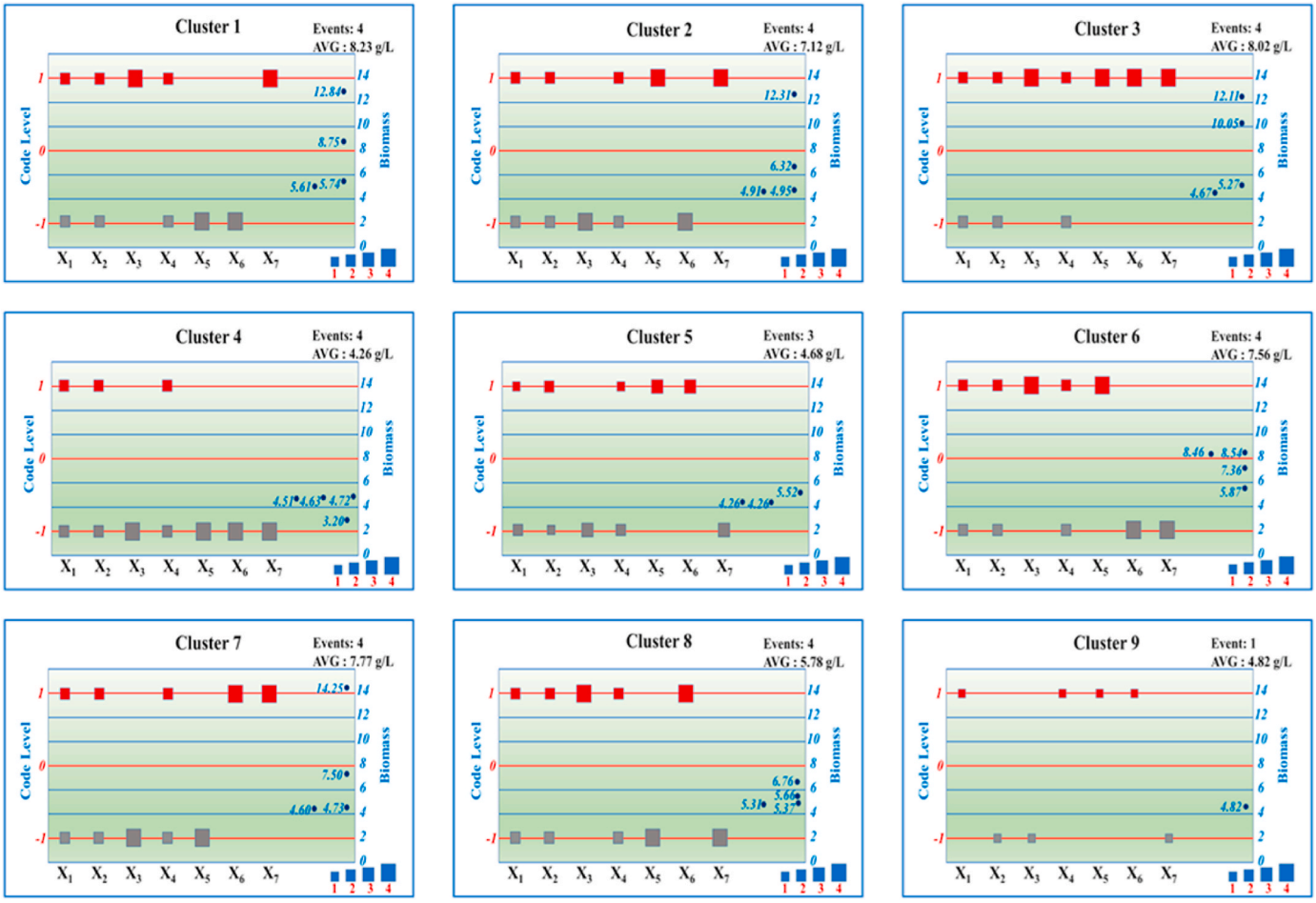

Fig. 4. Mean values of biomass production in Clusters 1–9 and the occurrence frequencies of input data (X_1–X_7) in the corresponding code levels. The larger the size of rectangle, the higher the frequency of events.

Table 2
Regression analysis of the fractional factorial design (T1).

Coefficients	Estimate	Std. Error	t value	Probability	
(Intercept)	−5.7475	1.58745	−3.621	0.00049	***
X_1	1.58864	0.21997	7.222	1.58E-10	***
X_2	0.03658	0.01106	3.307	0.00136	**
X_3	0.07014	0.02212	3.171	0.00208	**
X_4	−0.0822	1.38267	−0.059	0.95274	
X_5	1.5935	0.22123	0.72	0.4732	
X_6	−0.0124	0.02212	−0.562	0.5753	
X_7	0.54593	0.11061	4.935	3.65E-06	***

***: $p < 0.001$; **: $p < 0.01$; *: $p < 0.05$; R-Squared: 0.5155.

3.3. Steepest ascent method (SAM) for identifying the search direction

SAM is conducted by searching the direction of the steepest ascent and moving the maximal response value toward the neighborhood of the optimum process response, where experiments are conducted until there is no further increase in the response [46]. This model is useful in indicating the direction along which variables keep changing in order to enhance mycelial biomass (Yieldmax (Eq. (3)). The path of steepest ascent can be determined using Eq. (3).

From the regression analysis, the probability of significance showed X_1 (pH), X_2 (glucose), X_3 (PDB) and X_7 (agar) significantly impacted the biomass, whereas X_4 (CC-PS), X_5 (camphor) and X_6 (CC water extract) had no significant impacts on the biomass (Table 2). Therefore, X_1 (pH), X_2 (glucose), X_3 (PDB) and X_7 (agar) that showed a relatively significant contribution to the biomass were used in SAM. Hence, the path of

Table 3
Assigned concentration of each variable at different code levels and the results of the path of the steepest ascent experiment (T2).

Factor	PH	Glucose	PDB	CC PS	Camphor	CC water extract	Agar	Yield (g/L)[a]
		g/L						
−2	3.1107	19.13	39.17	0.16	1	20	0.7	3.22 ± 0.08
−1	4.0553	19.56	39.58	0.16	1	20	1.35	2.60 ± 0.08
0	5	20	40	0.16	1	20	2	5.31 ± 1.11
1	5.9447	20.44	40.42	0.16	1	20	2.65	6.89 ± 0.37
2	6.8893	20.87	40.83	0.16	1	20	3.3	7.77 ± 0.93
3	7.834	21.32	41.26	0.16	1	20	3.95	5.84 ± 0.83

[a] Under the condition of 28 °C and 50 rpm for 7 days. N = 3 (repeated 3 times under same experimental condition).

steepest ascent was designed to keep the other non-significant factors (not significant at a 95% confidence interval) at the center point level of the PBD space. SAM was used to estimate the coefficients of the first-order approximation. In code forms, X_1 (pH), X_2 (glucose), X_3 (PDB) and X_7 (agar) were increased by 0.94467, 0.02175, 0.04171 and 0.32463 units, respectively (Table 4). Based on Eq. (3), Table 3 showed the direction along which the variables kept changing. SAM verified how the biomass changed systematically when the variables were systematically altered as per Eq. (3) using predetermined increments. There were six experiments in this section. The composition of the path of steepest ascent experiment (T2) was at the second-code level, and the following experimental compositions increased at a specific constant rate based on the coefficients of X_1, X_2, X_3 and X_7 listed in Supplementary Tables S–2**.** It can be concluded from Table 3 that increasing the value of pH and the concentrations of glucose, PDB and agar by two units could result in the maximal increase (7.77 g/L) in the response (biomass), and therefore this code level was used as the star point of CCDs to estimate curvature. After that, the biomass decreased (the third-code level resulted in a yield of 5.84 g/L). It reveals the concentration of each factor approaching the range where the extreme point was located was at around two units of the star point. This study used this point (the code level of +2 in Table 3) as the center point of CCD.

3.4. Central composite design (CCD) model fitting

An experimental design was formulated, whose center point was moved in the direction of the condition giving the highest growth response on the steepest path. CCD was used to analyze the concentrations of the variables (media components and pH) suitable for the biomass production of *A. cinnamomea* and the experimental domain depicting the levels and interactions between the biomass and each selected variable to fit into a regression equation. CCD began with a fractional factorial design (with center points) and added "star" points to estimate the curvature. The concentration ranges and pH values of X_1 (pH), X_2 (glucose), X_3 (PDB) and X_7 (agar) were determined based on the results reported in the section of SAM and the concentration ranges adopted in the PBD and in the unoptimized media [17]. The concentrations of all the other factors (X_4 (CC-PS), X_5 (camphor) and X_6 (CC water extract)) were maintained at the center point level. Therefore, the experimental design was formulated, where a center point moved in the direction of the condition giving the highest growth response on the steepest path. The experiment's domain that was out of the initial domain was rearranged to proceed further in CCD (Supplementary Tables S–4**)**.

This study consisted of a 26-run fractional factorial design. Second-order coefficients were assessed for estimating the 15 coefficients of the model. The statistical software package, JMP statistical software package (SAS Institute Inc., USA), was used to perform the 26-run fractional factorial design that comprised four variables (X_1, X_2, X_3 and X_7), varying at five different code levels, i.e. very high (+2), high (+1), 0, low (−1), and very low (−2). The 26 runs in the design were composed of 16 cubic (factorial) points, 2 replicates of the center point, and 8 axial (star) points. The various levels of the factor matrix and the yields of mycelia under different combinations of X_1 (pH), X_2 (glucose), X_3 (PDB) and X_7 (agar) after 7 days of fermentation are given in Table 4.

The experimental data of CCD were fitted using a polynomial equation including the second-order regression (Eq. (1)) to determine the coefficient and the *p* value of each variable (Table 5). The final regression equation in terms of code values (Eq. (1)) was expressed with actual values (Eq. (4)), and therefore Y (the biomass after 7-day incubation) was predicted. The values of X_1 (pH), X_2 (glucose), X_3 (PDB) and X_7 (agar) were therefore obtained **(**Supplementary Tables S–3**).**

$$Y = -2698.3713 + 55.6831X_1 + 6.0232X_2 + 114.4838X_3 + 70.9194X_7 - 0.5696X_1X_2 - 0.7760X_1X_3 - 1.1495X_1X_4 - 1.1598X_2X_3 + 0.2945X_2X_7 - 1.4737X_3X_7 - 0.5716X_1^2 + 1.0578X_2^2 - 0.9827X_3^2 - 1.2911X_7^2 \quad (4)$$

where X_1, X_2, X_3, and X_7 denoted the code values of the four test variables (i.e., pH, concentration of glucose, PDB, and agar, respectively).

The *p* values shown in Table 5 indicate X_1 (pH), X_3 (PDB) and X_7 (agar) are the crucial factors affecting the value of Y while X_2 (glucose) has no significant effect on the value of Y. Besides, the interactions of X_1 and X_7 are important, similarly for those of X_3 and X_7.

To resolve the maximization problem by partial differentiation, a local maximum was presented.

$$\frac{\partial Y}{X1} = a_1 + 2a_{11}X_1 + a_{12}X_2 + a_{13}X_3 + a_{17}X_7 \quad (5.1)$$

$$\frac{\partial Y}{X2} = a_2 + a_{12}X_1 + 2a_{22}X_2 + a_{23}X_3 + a_{27}X_7 \quad (5.2)$$

$$\frac{\partial Y}{X3} = a_3 + a_{13}X_1 + a_{23}X_2 + 2a_{33}X_3 + a_{37}X_7 \quad (5.3)$$

Table 4
Experimental design and results of CCD at B85 T3 experiment of 26 runs.

Run[a]	pH	Glucose	PDB	Agar	Experimental yield
	Code level				(g/L)
1	1	1	1	1	4.800
2	1	1	1	−1	5.907
3	1	1	−1	1	5.047
4	1	1	−1	−1	5.633
5	1	−1	1	1	5.540
6	1	−1	1	−1	7.847
7	1	−1	−1	1	8.400
8	1	−1	−1	−1	6.190
9	−1	1	1	1	9.213
10	−1	1	1	−1	5.117
11	−1	1	−1	1	8.443
12	−1	1	−1	−1	5.300
13	−1	−1	1	1	7.033
14	−1	−1	1	−1	6.853
15	−1	−1	−1	1	8.753
16	−1	−1	−1	−1	5.290
17	2	0	0	0	8.050
18	−2	0	0	0	2.450
19	0	2	0	0	8.610
20	0	−2	0	0	7.603
21	0	0	2	0	7.030
22	0	0	−2	0	6.170
23	0	0	0	2	4.237
24	0	0	0	−2	5.980
25	0	0	0	0	10.110
26	0	0	0	0	5.340

[a] All other media components were at center point of the PBD space.

Table 5
Parameter of the second-order regression based on the data of central composite designed experiments.

Independent variable	Coefficient estimate	t-value	*p*-value
a0	−2698.02	−0.6368	0.5265
a1	55.679	1.2854	0.2033
a2	6.015	0.0529	0.9580
a3	114.472	0.6654	0.5082
a7	70.919	1.1302	0.2627
a12	−0.57	−0.6317	0.5298
a13	−0.776	−0.8216	0.4144
a17	−1.15	−1.8834	0.0643
a23	−1.16	−0.5721	0.5693
a27	0.295	0.2248	0.8228
a37	−1.474	−1.0738	0.2870
a11	−0.572	−1.4230	0.1597
a22	1.058	0.5681	0.5720
a33	−0.983	−0.4819	0.6315
a77	−1.291	−1.5206	0.1334

$$\frac{\partial Y}{X7} = a_7 + a_{17}X_1 + a_{27}X_2 + a_{37}X_3 + 2a_{77}X_7 \quad (5.4)$$

The maximum biomass of mycelia was achieved theoretically at initial pH (7.39), glucose (20.83 g/L), PDB (40.44 g/L) and agar (3.47 g/L). To prove its feasibility, three replications with the optimum medium were carried out, with an average biomass of 9.70 g/L. The optimum concentration and the results of biomass production are shown in Fig. 5.

3.5. Predicted optimal biomass production by RSM

It is important to justify whether RSM could accurately identify the medium conditions resulting in the optimal biomass production. Therefore, the performance of biomass production predicted by RSM design was verified by the experimental results. Using a medium composition located within the optimal range i (the cultural 7.39 of pH value, 20.83 g/L of glucose, 40.44 g/L of PDB, 0.16 g/L of CC-PS, 1 g/L of camphor, 20 g/L of CC water extract, and 3.47 g/L of agar), the results from the confirmation experiments gave a biomass value (Y) of 9.70 ± 0.60 g/L (Fig. 5). The yield of RSM was 200% higher than that (4.72 ± 0.33 g/L) of the control medium, indicating the response surface analysis was indeed an effective tool for improving biomass production. Moreover, the best performance of biomass production obtained from this work is also higher than that of the maximum (7.7 g/L) in Table 3.

In most fungal biomass studies, a relatively high C/N (carbon to nitrogen) ratio was favorable for mycelial growth [47] and carbon substrate is considered the most important performance index for biomass production. It was reported that the availability of monosaccharide was better than that of disaccharide, and glucose concentration had the most impact on the mycelial production of *A. cinnamomea* [48]. Both the RSM and SOM results obtained from this study indicated both PDB (X_3) and agar (X_7) were more important carbon sources than glucose (X_2), where the carbon source was selected based primarily on mono- and di-saccharides. According to this study, the high biomass value indicated the effectiveness of converting carbon substrate (PDB and agar) into biomass production. Hence, the response surface analysis was also conducted to investigate the interactive effects of PDB and agar on the yield. The results showed the interactions between PDB and agar were important to the yield (Eq. (4)). In this study, pH appeared to have a minimal impact on the culture system. The initial pH was designed to range from 5 to 8.77 (Supplementary Tables S–4), and the optimum pH was determined to be 7.39. RSM was also used to optimize the medium composition for the enhancement of biomass productivity of *A. cinnamomea* [4]. The inference that pH played a crucial role in biomass production was also observed [49]. The optimal initial pH value of 5.54 together with 4.78 g/100 mL of corn powder, 3.19 g/100 mL of yeast malt broth reached the maximal biomass production. The different strains of the fungus and carbohydrate components used in RSM may result in different optimal initial pH values in this study.

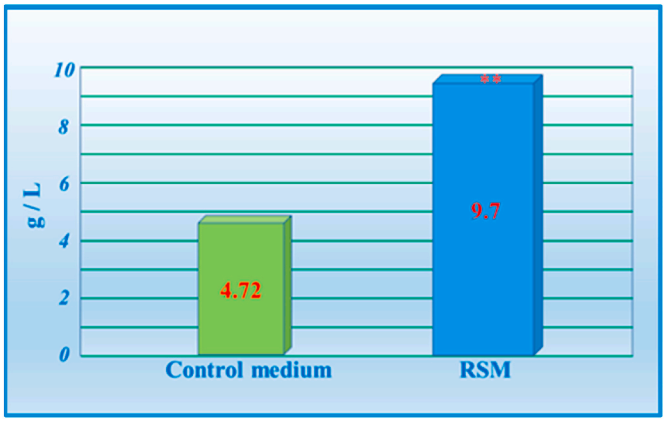

Fig. 5. Biomass production of *A. cinnamomea* under RSM and control medium conditions. $^{**}p < 0.01$, compared with control.

3.6. Experimental validation of RSM and ANN responses

The optimum culture condition obtained from RSM for achieving the highest biomass production of *A. cinnamomea* was found to be 7.39 of pH, 20.83 g/L of glucose, 40.44 g/L of PDB, 0.16 g/L of CC-PS, 1 g/L of camphor, 20 g/L of CC water extract, and 3.47 g/L of agar based on a given set of reaction parameters. Experiments were carried out in triplicate, along with the control medium (the initial point). The biomass value of RMS was 9.70 ± 0.60 g/L, while the biomass value of the control medium was 4.72 ± 0.33 g/L (Fig. 5), indicating a more than 200% increase in biomass production made by RSM. This suggests RSM is a more successful statistical design for the optimization of multiple factors at a small test scale, compared with the one-factor-at-a-time test.

The response surface analysis was further conducted to examine the interactive effects of PDB and agar on the yield. Several studies indicated the extent of X_3 (PDB) and X_7 (Agar) based on the response surface model established for Yieldmax (Eqs. (1), (2) and (4)), and the optimal operating condition was obtained. Since the performance indexes of pH (X_1), glucose (X_2), PDB (X_3), and agar (X_7) indicated they were key factors from RSM, it would be of great interest to reveal the global optimum leading to the best overall ability of a multi-factor system for biomass production.

According to RSM, this study conducted 4-stage experiments (T1-T4), including 96 runs in the first stage (32 conditions, and repeated 3 times), 18 runs in the second stage (6 conditions, and repeated 3 times), 78 runs in the third stage (26 conditions, and repeated 3 times), and 6 runs in the fourth stage (2 conditions, and repeated 3 times). It is worth noting that the results of SOM based on the first-stage results (T1) of RSM pointed out the dominance of X_3 and X_7 in the growth of *A. cinnamomea*, and RSM also obtained the same results. This recommends the applicability and practicability of ANN in determining the dominant factors for biomass production in a rather efficient way, which can be cost-effective and less laborious in support of RSM.

In sum, the proposed model hybriding RSM and ANN is suitable for relating the mycelial biomass with initial pH, glucose, PDB and agar, and the computation-based optimization results can be applicable to the liquid culture process to enhance the yield of *A. cinnamomea*.

4. Conclusion

This study developed a hybrid methodology integrating ANN and RSM to optimize the culture condition of *A. cinnamomea,* where ANN was used to efficiently and effectively identify the dominant factors for biomass production and RSM was used to explore the optimum conditions for the process response.

The ANN-based SOM clustering analysis of the first-stage results of RSM suggested PDB and agar are the desired dominant factors. A maximum yield of 9.70 g/L (200% increase in biomass, compared to that of the control medium) was observed under RSM conditions over 7 days at 28 °C, which is better than those of the documented reports in the literature. The results indicate that statistical approach of the experimental design is effective in enhancing yield. Besides, PDB and agar as well as their interactions are the crucial factors affecting biomass production, which conform to SOM results.

The hybrid ANN & RSM methodology established in this study can obtain a favorable composition of carbohydrate-based substrates and pH in culture to improve biomass production significantly. These findings will surely aid in developing a commercially viable way for biomass production of other biomaterials in an economical process.

E-supplementary Tables of this work can be found in online version of the paper.

Data availability

The full data supporting the findings of this study are available in the Tables.

Acknowledgements

This work was supported by grants from the Ministry of Science and Technology, Taiwan (MOST 108-2320-B-077-005-MY3 to MKL; MOST 107-2621-M-002-004-MY3 to FJC).

Appendix A. Supplementary data

Supplementary data to this article can be found online at https://doi.org/10.1016/j.biombioe.2022.106349.

References

[1] M. Destek, S. Sarkodie, A. Esamoah, Does biomass energy drive environmental sustainability? An SDG perspective for top five biomass consuming countries, Biomass Bioenergy 149 (2021) 106076.
[2] C. Chiang, B. Chiang, Processing characteristics of submerged fermentation of *Antrodia cinnamomea* in airlift bioreactor, Biochem. Eng. J. 73 (2013) 65–71.
[3] T. Ma, Y. La, L. Chen, F. Yang, The cultivation strategy of enhancing triterpenoid production in submerged cultures of *Antrodia cinnamomea* by adding monoterpenes, J. Taiwan Inst. Chem. Eng. 58 (2016) 210–218.
[4] F. Yang, U. Yang, H. Lu, Enhanced antioxidant and antitumor activities of *Antrodia cinnamomea* cultured with cereal substrates in solid state fermentation, Biochem. Eng. J. 78 (2013) 108–113.
[5] N. Hassan, S. Supramani, M. Sohedein, S. Usuldin, A. Klaus, Z. Ilham, W. Chen, W. Wan-Mohtar, Efficient biomass-exopolysaccharide production from an identified wild-Serbian *Ganoderma lucidum* strain BGF4A1 mycelium in a controlled submerged fermentation, Biocatal. Agric. Biotechnol. 21 (2019) 101305.
[6] J. Lee, W. Jung, S. Park, K. Lee, W. Shin, E. Hong, Culture conditions and medium components for the production of mycelial biomass and exo-polysaccharides with *Paecilomyces japonica* in liquid culture, J. Biosci. Bioeng. 115 (2013) 433–437.
[7] K. Lee, M. Zanil, K. Chan, Z. Chin, Y. Liu, S. Lim, Synergistic ltrasound-assisted organosolv pretreatment of oil palm empty fruit bunches for enhanced enzymatic saccharification: an optimization study using artificial neural networks, Biomass Bioenergy 139 (2020) 105621.
[8] H. Long, C. Hu, C. Weng, *Antrodia cinnamomea* prolongs survival in a patient with small cell lung cancer, Medicina 55 (2019) 640.
[9] D. Tsai, C. Chung, K. Lee, *Antrodia cinnamomea* induces autophagic cell death via the CHOP/TRB3/Akt/mTOR pathway in colorectal cancer cells, Sci. Rep. 8 (2018) 1–12.
[10] Y. Jin, H. Liu, J. Liu, H. Xing, F. Wang, L. Deng, Efficient production of 4-Acetylantroquinonol B from *Antrodia cinnamomea* through two-stage carbon source coordination optimization, Bioresour. Technol. Rep. 15 (2021) 100732.
[11] T. Lin, A. Tseng, C. Chao, M. Lu, Microelements induce changes in characterization of sulfated polysaccharides from *Antrodia cinnamomea*, Int. J. Biol. Macromol. 120 (2018) 952–958.
[12] T. Lin, C. Chang, A. Tseng, C. Chao, M. Lu, Sodium thiosulfate enhances production of polysaccharides and anticancer activities of sulfated polysaccharides in *Antrodia cinnamomea*, Carbohydr. Polym. 216 (2019) 204–212.
[13] M. Lu, M. Lee, C. Chao, Y. Hsu, Physiochemical changes and mechanisms of anti-inflammation effect of sulfated polysaccharides from ammonium sulfate feeding of *Antrodia cinnamomea*, Int. J. Biol. Macromol. 148 (2020) 715–721.
[14] M. Lu, T. Lin, C. Chang, Chemical identification of a sulfated glucan from Antrodia cinnamomea and its anti-cancer functions via inhibition of EGFR and mTOR activity, Carbohydr. Polym. 202 (2018) 536–544.
[15] N. Huang, J. Cheng, W. Lai, M. Lu, *Antrodia camphorata* prevents rat pheochromocytoma cells from serum deprivation-induced apoptosis, FEMS Microbiol. Lett. 244 (2005) 213–219.
[16] I. Lee, R. Huang, C. Chen, H. Chen, W. Hsu, M. Lu, *Antrodia camphorata* polysaccharide exhibits anti-hepatitis B virus effects, FEMS Microbiol. Lett. 209 (2002) 63–67.
[17] Y. Shen, C. Chou, Y. Wang, C. Chen, C.Y. Chou, M. Lu, Anti-inflammatory activity of the extracts from mycelia of *Antrodia camphorata* cultured with water-soluble fraction from five different *Cinnamomum genera*, FEMS Microbiol. Lett. 231 (2004) 137–143.
[18] G. Box, K. Wilson, On the experimental attainment of optimum conditions, J. Royal Stat. Soc. A (General). 13 (1951) 1–45.
[19] M. Prakash, V. Sivakumar, R. Sridhar, I. Prince, Development of model for mechanical properties of tapioca starch based films, Ind. Crop. Prod. 42 (2013) 159–168.
[20] R. Triveni, T. Shamala, N. Rastogi, Optimised production and utilization of exopolysaccharide from *Agobacterium radiobacter*, Process Biochem. 36 (2001) 787–795.
[21] N. Kumar, M. Rajarathinam, K. Muthuvelu, T. Senniyappan, New insight into the effect of fungal mycelia present in the bio-pretreated paddy straw on their enzymatic saccharification and optimization of process parameters, Bioresour. Technol. 267 (2018) 291–302.
[22] T. Senthivelan, J. Kanagaraj, R. Panda, T. Narayani, Screening and production of a potential extracellular fungal laccase from *Penicillium chrysogenum*: media optimization by response surface methodology (RSM) and central composite rotatable design (CCRD), Biotechnol. Rep. 23 (2019), e00344.
[23] M. Yadav, V. Vivekanand, Biological treatment of lignocellulosic biomass by *Curvularia lunata* for biogas production, Bioresour. Technol. 306 (2020) 123151.
[24] O. Obafemi, A. Stephen, O. Ajayi, M. Nkosinathi, A survey of artificial neural network-based prediction models for thermal properties of biomass, Procedia Manuf. 33 (2019) 184–191.
[25] R. Özçelık, M. Diamantopoulou, J. M, M. Eker, N. Gürlevık, Artificial neural network models: an alternative approach for reliable aboveground pine tree biomass prediction, For. Sci. 63 (3) (2017) 291–302.
[26] O. Yucel, E.S. Aydin, H. Sadikoglu, Comparison of the different artificial neural networks in prediction of biomass gasification products, Int. J. Energy Res. 43 (11) (2019) 5992–6003.
[27] S. Dahunsi, S. Oranusi, V. Efeovbokhan, Pretreatment optimization, process control, mass and energy balances and economics of anaerobic co-digestion of *Arachis hypogaea* (Peanut) hull and poultry manure, Bioresour. Technol. 241 (2017) 454–464.
[28] K. Naresh, R. Ravikumar, S. Kirupa, S. Thenmozhi, New insight into the effect of fungal mycelia present in the bio-pretreated paddy straw on their enzymatic saccharification and optimization of process parameters, Bioresour. Technol. 267 (2018) 291–302.
[29] L. Chang, F. Chang, S. Yang, F. Tsai, T. Chang, E. Herricks, Self-organizing maps of typhoon tracks allow for flood forecasts up to two days in advance, Nat. Commun. 11 (2020) 1–13.
[30] I. Chen, L. Chang, F. Chang, Exploring the spatio-temporal interrelation between groundwater and surface water by using the self-organizing maps, J. Hydrol. 556 (2018) 131–142.
[31] P. Kow, Y. Wang, Y. Zhou, I. Kao, M. Issermann, L. Chang, F. Chang, Seamless integration of convolutional and back-propagation neural networks for regional multi-step-ahead PM2. 5 forecasting, J. Clean. Prod. 261 (2020) 121285.
[32] Y. Zhou, F.J. Chang, H. Chen, H. Li, Exploring copula-based Bayesian model averaging with multiple ANNs for PM2. 5 ensemble forecasts, J. Clean. Prod. 263 (2020) 121528.
[33] M. Ozonoh, B.O. Oboirien, M.O. Daramola, Optimization of process variables during torrefaction of coal/biomass/waste tyre blends: application of artificial neural network & response surface methodology, Biomass Bioenergy 143 (2020) 105808.
[34] D. Baruah, D.C. Baruah, M.K. Hazarika, Artificial neural network based modeling of biomass gasification in fixed bed downdraft gasifiers, Biomass Bioenergy 98 (2017) 264–271.
[35] N. Dave, T. Varadavenkatesan, R. Selvaraj, R. Vinayagam, Modelling of fermentative bioethanol production from indigenous *Ulva prolifera* biomass by Saccharomyces cerevisiae NFCCI1248 using an integrated ANN-GA approach, Sci. Total Environ. 791 (2021) 148429.
[36] T. Suresh, N. Sivarajasekar, K. Balasubramani, T. Ahamad, M. Alam, M. Naushad, Process intensification and comparison of bioethanol production from food industry waste (potatoes) by ultrasonic assisted acid hydrolysis and enzymatic hydrolysis: statistical modelling and optimization, Biomass Bioenergy 142 (2020) 105752.
[37] M. Ozonoh, B.O. Oboirien, M.O. Daramola, Optimization of process variables during torrefaction of coal/biomass/waste type blends: application of artificial neural network & response surface methodology, Biomass Bioenergy 143 (2020) 105808.
[38] Z. Wang, X. Peng, A. Xia, A. Shah, Y. Huang, X. Zhu, X. Zhu, Q. Liao, The role of machine learning to boost the bioenergy and biofuels conversion, Bioresour. Technol. 343 (2022) 126099.
[39] S. Sheu, C. Chen, C. Chen, Study on the host specificity of *Antrodia camphorata*, Taiwan. J. Agric. Chem. Food Sci. 38 (2000) 533–539.
[40] P. Ghosh, S. Mukherji, Optimization of media composition for enhancing carbazole degradation by *Pseudomonas aeruginosa* RS1, J. Environ. Chem. Eng. 6 (2018) 2881–2891.
[41] T. Kohonen, Self-organized formation of topologically correct feature maps, Biol. Cybern. 43 (1982) 59–69.
[42] A. Adeloye, R. Rustum, I. Kariyama, Neural computing modeling of the reference crop evapotranspiration, Software 29 (2012) 61–73.
[43] L. Chang, W. Wang, F. Chang, Explore training self-organizing map methods for clustering high-dimensional flood inundation maps, J. Hydrol. 595 (2021) 125655.
[44] T. Kohonen, The self-organizing map, Proc. IEEE 78 (1990) 1464–1480.
[45] S. Rout, S. Das, In vitro manipulation and propagation of medicinal plants, Biotechnol. Adv. 18 (2000) 91–120.
[46] R. Gheshlaghi, J. Scharer, M. Moo-Young, P. Douglas, Medium optimization for hen egg white lysozyme production by recombinant *Aspergillus niger* using statistical methods, Biotechnol. Bioeng. 90 (2005) 754–760.
[47] E. Lin, Y. Chen, Factors affecting mycelial biomass and exopolysaccharide production in submerged cultivation of *Antrodia cinnamomea* using complex media, Bioresour. Technol. 98 (2007) 2511–2517.
[48] L. Chen, Z. Wang, B. Zhang, M. Ge, H. Ng, Y. Niu, L. Liu, Production, structure and morphology of exopolysaccharides yielded by submerged fermentation of *Antrodia cinnamomea*, Carbohydr. Polym. 205 (2019) 271–278.
[49] F. Yang, H. Huang, M. Yang, The influence of environmental conditions on the mycelial growth of *Antrodia cinnamomea* in submerged cultures, Enzym. Microb. Technol. 33 (2003) 395–402.